

## Analog based pharmacophore strategy to identify novel leukotriene a4 hydrolase (LTA4H) inhibitors

Kranthi Raj K.<sup>1,4</sup>, Pathak L.P.<sup>4,5</sup>, \*Muttineni Ravikumar<sup>2,3</sup>, Ramachandran D.

<sup>1</sup>Acharya Nagarjuna University, P.G center, Nuzvid, 521201, Andhra Pradesh, India

<sup>2</sup>Bioinformatics Division, Environmental Microbiology Lab, Department of Botany, Osmania University, Hyderabad 500007, Andhra Pradesh, India

<sup>3</sup>Ravambio, Begumpet, Hyderabad 500016, Andhra Pradesh, India

<sup>4</sup>Biocampus, GVK Biosciences, S-1, Phase-1, Technocrats Industrial Estate, Balanagar, Hyderabad 500 037, Andhra Pradesh, India

<sup>5</sup>National Institute of Pharmaceutical Education and Research (NIPER), Hyderabad 5000 37, Andhra Pradesh, India

**Abstract-** Leukotriene A4 hydrolase (LTA4H) is a hydrolase with a bifunctional zinc enzyme, which plays a role in inflammation. LTA4H may also play an important role in carcinogenesis, especially chronic inflammation-associated carcinogenesis. In this study, chemical feature based pharmacophore models based on 22 currently available LTA4H inhibitors have been developed with the aid of HipHop and HypoRefine modules within Catalyst program package. 3D pharmacophore model developed was, characterized by distinct chemical features such as Hydrogen-bond acceptor (HA), Hydrogen-bond donor (HD), Hydrophobic aliphatic (HPAl), Hydrophobic aromatic (HPAr) that are found to be responsible for the activity of the LTA4H inhibitors. The correlation coefficient, root mean square deviation and cost difference were 0.92, 1.0867 and 53.62 respectively, suggesting that a highly predictive pharmacophore model was successfully obtained. The results of our study provide a valuable tool in designing new leads with desired biological activity for virtual screening.

**Key Words:** Leukotriene A4 hydrolase (LTA4H), Pharmacophore

### Introduction

Leukotriene A4 Hydrolase as a potent inhibitor in inflammation and cancer [1-3] Leukotriene A4 hydrolase, also known as LTA4H is a human gene. The protein encoded by this gene, a bifunctional zinc enzyme converts leukotriene A4 to leukotriene B4 (LTB4). LTA4H may play an important role in carcinogenesis, especially chronic inflammation associated carcinogenesis by two ways a) The inflammation augmenting effect of inflammatory cells b) The autocrine growth-stimulatory effect of LTB4 produced by epithelial cells and the paracrine growth stimulatory effect of LTB4 produced by inflammatory cells, on pre-cancerous and cancer cells. Many drugs like Bestatin (N-[(2S,3R)-3-amino-2-hydroxy-4-phenyl-butanoyl]-L-leucine), Thioamine (3-(4-benzyloxyphenyl)-2-(R)-amino-1-propane thiol)hydroxamic acid((N-hydroxy-N-[(2S)-2-amino-3-(benzyloxyphenyl)propyl]-5-carboxypentanamide) are available in the market which inhibits hydrolase activity. The variability in potency found in LTA4H inhibitors (IC50 ranging

from sub-micromolar to high micromolar values for structurally related molecules) suggests that accessory binding pockets in the enzyme active site must be present and play a pivotal, still unclarified role in determining the affinity. It is therefore conceivable that the identification of such areas can be exploited for the design of novel, more potent LTA4H inhibitors. In view of the potential therapeutic importance of LTA4H inhibitors, we engaged ourselves in a program devoted to design feature based three-dimensional pharmacophore model for LTA4H inhibitors. In this frame, we report a molecular modeling study aimed at mapping the topography of the active site of LTA4H and at identifying the structural requirement for LTA4H inhibition. Many LTA4H inhibitors for which biological values are available were collected from the literature along with their inhibitory IC50 values. The Generated model can be further utilized for developing new potentially active candidates targeting LTA4H, which can be useful as anti inflammation agents.

### Methodology

For the pharmacophore modeling studies, a set of LTA4H inhibitory activity data (IC50) spanning over 4 orders of magnitude (from 1 to 630,000 nM) were selected [8-13]. The dataset was divided into training set (Insert Fig 1) and test set (supplementary information Table1). Some inactive compounds were also included in order to obtain critical information on pharmacophore requirements. The important aspect of this selection scheme was that each active compound would teach something new to the HypoGen module to help it cover as much critical information as possible for predicting biological activity. To generate 3D pharmacophore, each compound should have conformations to cover

Based on the resolution and the interaction of the co-crystallized ligand in the protein hydrolase and zinc domain part, X-ray crystallographic structure of protein having PDB ID 2VJ8 (with the resolution of 1.80 Å) has been selected from protein data bank [4] for the study, all the molecules were built using builder module of Cerius2 [5] and minimized using the steepest descent algorithm with a convergence gradient value of 0.001 kcal/mol. Docking was done to analyze the ligand-protein interaction with CDOCKER [6]. Pharmacophore generation was done in Catalyst 4.10 program [7].

### Pharmacophore Generation

three dimensional spaces. For this, conformational models of all molecules were generated using the 'best quality' conformational search option within the Catalyst's ConFirm module. It generates the conformations using the Poling' algorithm [14]. A maximum of 250 conformations were generated for each compound to ensure maximum coverage in the conformational space within default energy threshold of 20 kcal/mol above the global energy minimum. Ten best Pharmacophore (called hypotheses in the program) models were generated using HypoGen module. An initial analysis revealed that four chemical feature types such as hydrogen-bond acceptor (HA), hydrogen-bond donor (HD), hydrophobic aliphatic (HPAl), hydrophobic aromatic (HPAr) features could effectively map all critical chemical features of all molecules in the training and test sets. These features were selected and used to build a series of hypotheses using default uncertainty value 3 (defined by Catalyst as the measured value being within three times higher or three times lower of the true value). Indeed, Catalyst generates a chemical-feature-based model on the basis of the most active compounds. These compounds are determined by performing a simple calculation based on the activity and uncertainty. In hypothesis generation, the structure and activity correlations in the training set were rigorously examined. HypoGen identifies features that were common to the active compounds but excludes from the inactive compounds within conformationally allowable regions of space. It further estimates the activity of each training set compound using regression parameters. The parameters are computed by the regression analysis using the relationship of geometric fit value versus the negative logarithm of activity. Greater the geometric fit indicates greater activity prediction of the compound. The fit function does not only check if the feature is mapped or not, it also contains a distance term, which measures the distance that separates the feature on the molecule from the centroid of the hypothesis feature.

### Results and Discussion

The pharmacophore model has two hydrogen bond acceptor (HA), two hydrogen-bond donor (HD), and two hydrophobic aromatic (HPAr), (Insert Fig 2) Fig 2 shows the best hypothesis model Hypo 1 produced by the HypoGen module in Catalyst 4.10 software. (Insert Fig 3) Fig 3 shows the Hypo1 aligned with the highest active compound, and (Insert Fig 4) Fig 4 shows the Hypo1 aligned with the lowest active compound of the training set.

Fig 5 (Insert Fig 5) shows the Hypo1 aligned with the highest active compound, and Fig 6 shows the Hypo1 aligned with the lowest active compound of the test set. (Insert Fig 6) Results of pharmacophore hypotheses are presented in Table 1. (Insert Table 1) The first hypothesis (Hypo1) was the best pharmacophore hypothesis which is characterized by the highest cost difference (53.62), lowest root-mean-square error

(1.0867), and the best correlation coefficient (0.92) shown in Fig 7. (Insert Fig 7) The fixed cost and null cost are 91.1529 and 158.768 respectively. The generated pharmacophore model has predicted the activity of a large and diverse dataset of 168 test set compounds with correlation of 0.86. As we can see from Fig 3 & 5, activity of the compounds was predicted correctly. The features of the Hypo1 are fitting well to all the chemical features of highly active test set compounds.

Docking was performed using CDOCKER program with the highest and least active compounds (Table 2). (Insert Table 2) Highest active molecule which has been subjected to CDOCKER showing its interactions with Gln 136, Gly 268, Gly 269, Glu 271, His 295, Glu 271, Arg563 and His 299 amino acids of protein 2VJ8 shown in fig 8, with a docking score of -35.89 (Insert Fig 8) and lowest active molecule which has been subjected to CDOCKER showing its interaction with Ser295, Glu348, Asn291 and Lys565 amino acids of the protein 2VJ8 shown in fig 9, (Insert Fig 9) with a docking score of -13.68.

### Conclusion

The work in the catalyst presented in the study shows how chemical features hydrogen acceptor, hydrophobic aliphatic of set of compounds along with their activities ranging over several orders of magnitude can be used to generate pharmacophore hypothesis, that can successfully predict the biological activity. The models were not only predictive within the same series of compounds but different classes of diverse compounds also effectively mapped onto most of the features important for activity as they had a good correlation value of 0.92 and a good configuration cost value 13.45. The pharmacophore generated can be used for diversified structures that can be potentially inhibit LTA4H inhibitors discovery and to evaluate how well any newly designed compound maps in the pharmacophore developed in this study, using inhibitors against LTA4H showed distinct features that may be responsible for the activity of the inhibitors.

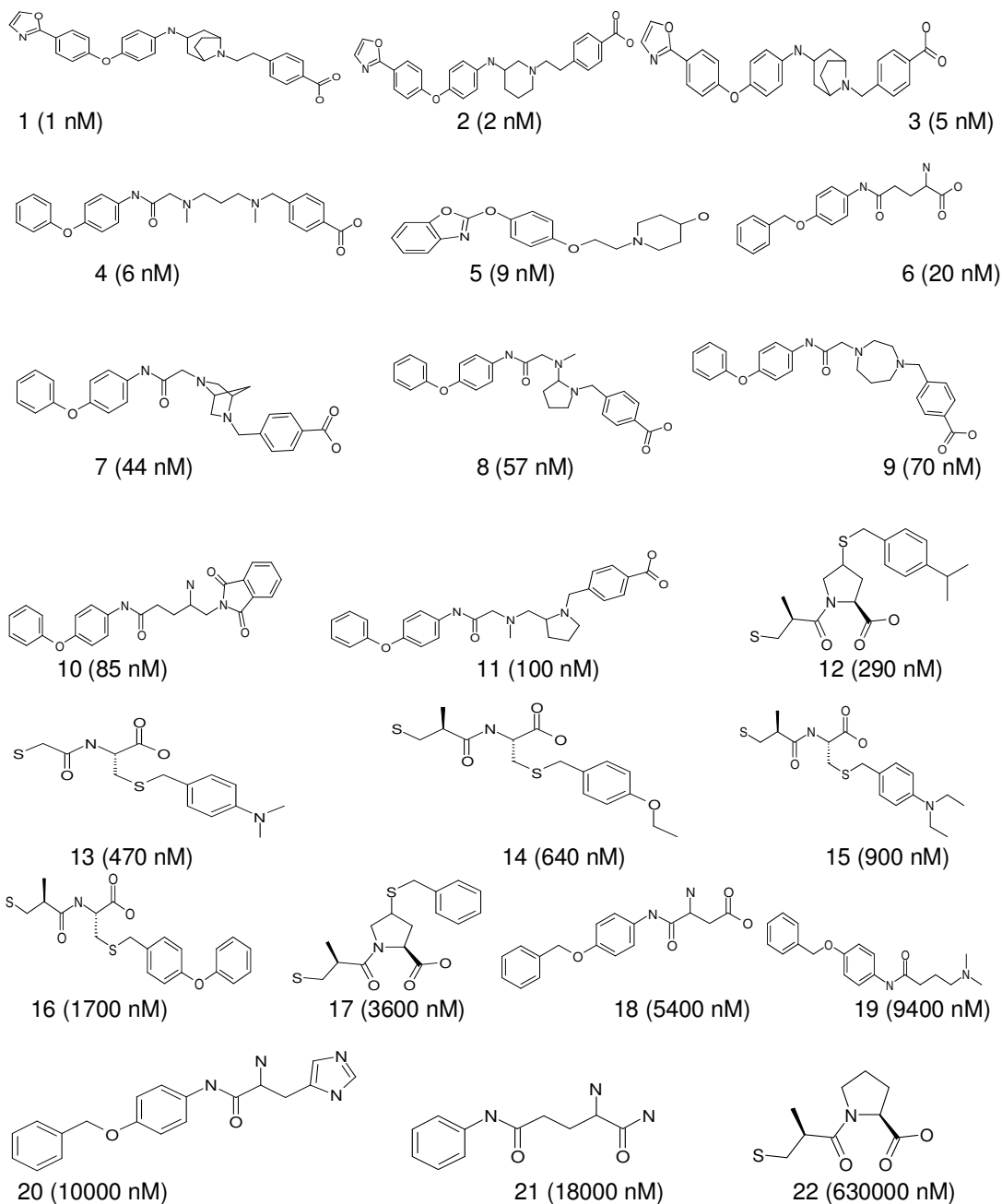
### Acknowledgements

We thank BIOCAMPUS, GVK Biosciences Pvt. Ltd., for providing software facilities.

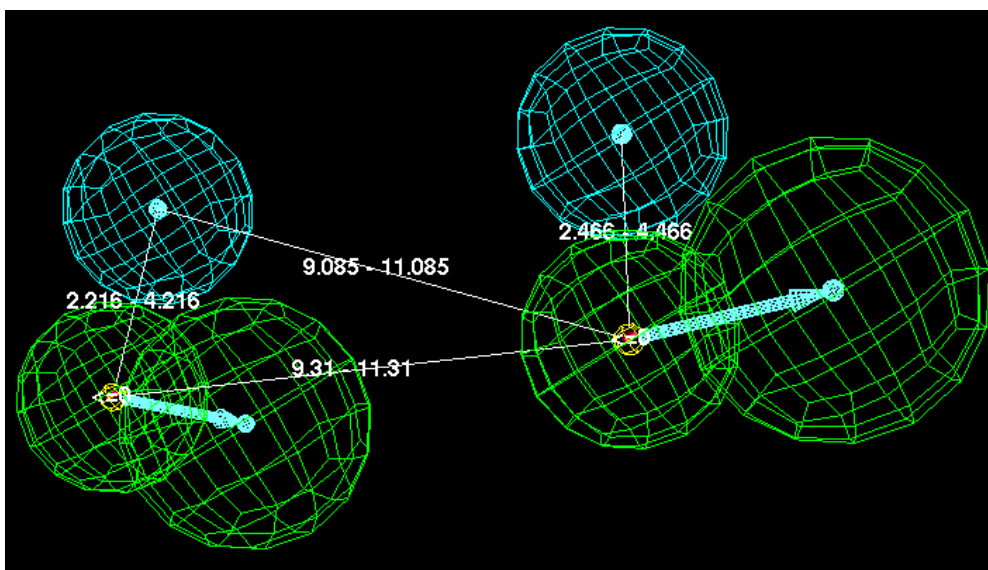
### References

- [1] Chen X., Wang S., Wu N., Yang C.S. (2004) *Current Cancer Drug Targets*, 4 (3), 267-283.
- [2] Bigby T.D., D. M. Lee., N. Meslier., D. C. Gruenert. (1989) *Biochemical and Biophysical Research Communications*, 164 (1), 1-7.
- [3] Zheng Sun., Sood,S., Ning L., Ramji D., Yang P., Newman R.A., Yang C. S. and Chen X. (2006) *Carcinogenesis*, 27 (9), 1902-1908.
- [4] Berman H. M., Westbrook J., Feng Z., Gilliland G., Bhat T. N., Weissig H.,

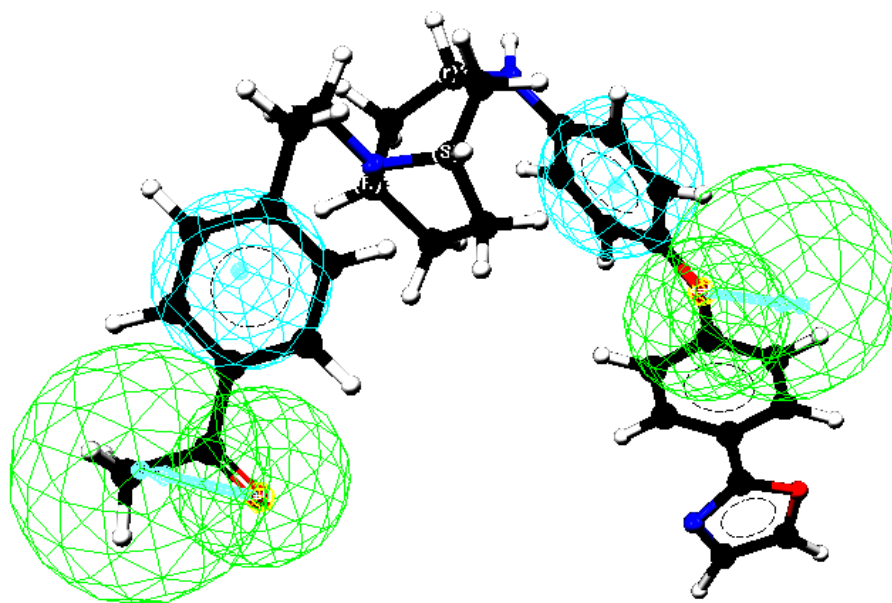
- Shindyalov I. N., Bourne P. E. (2000) *Nucleic Acids Res*, 28(1), 235-242.
- [5] Cerius 2, molecular modeling program package, Accelrys: San Diego, CA.
- [6] Wu G., Robertson D.H., Brooks C.L. Vieth M. (2003) *J Computational chemistry*, 24(13), 1549–1562
- [7] Catalyst v4.10. Molecular Simulations. San Diego, CA.
- [8] Grice C.A., Tays K.L., Savall B.M., Wei J., Butler C.R., Axe F.U., Bembenek S.D., Fourie A.M., Dunford P.J., Lundeen K., Coles F., Xue X., Riley J.P., Williams K.N., Karlsson L., Edwards J.P. (2008) *Journal of Medicinal Chemistry*, 51, 4150-4169.
- [9] Kirkland T. A., Adler M., Bauman J.G., Chen M., Haeggström J.Z., King B., Kochanny M. J., Liang A. M., Mendoza L., Phillips G.B., Thunnissen G. B., Trinh L., Whitlow M., Ye B., Ye H., Parkinson J., Guilford W. J. (2008) *Bioorganic & Medicinal Chemistry*, 16(9), 4963-4983
- [10] Bin Ye, Bauman J., Chen M., Davey D., Khim S.K., King B., Kirkland T., Kochanny M., Liang A., Lentz D., May K., Mendoza L., Phillips G., Selchau V., Schlyer S., Tseng J.L., Wei R.G., Ye H., Parkinson J., Guilford W.J. (2008) *Bioorganic & Medicinal Chemistry Letters* 18(14), 3891-3894
- [11] Khim S.K., Bauman J., Evans J., Freeman B., King B., Kirkland T., Kochanny M., Lentz D., Liang A., Mendoza L., Phillips G., Tseng J.L., Wei R.G., Ye H., Yu L., Parkinson J., Guilford W.J. (2008) *Bioorganic & Medicinal Chemistry Letters*, 18(14), 3895-3898
- [12] Enomoto H., Morikawa Y., Miyake Y., Tsuji F., Mizuchi M., Sahara H., Fujimura K.I., Horiuchi, M., Ban M. (2008) *Bioorganic & Medicinal Chemistry Letters* 18 (16), 4529-4532.
- [13] Enomoto H., Morikawa Y., Miyake Y., Tsuji F., Mizuchi M., Sahara H., Fujimura K.I., Horiuchi, M., Ban M. (2009), *Bioorganic & Medicinal Chemistry Letters*, 19 (2), 442-446
- [14] Smellie A., Teig S.L., Towbin P. (1995) *Journal of Computational Chemistry*, 16(2), 171–187.



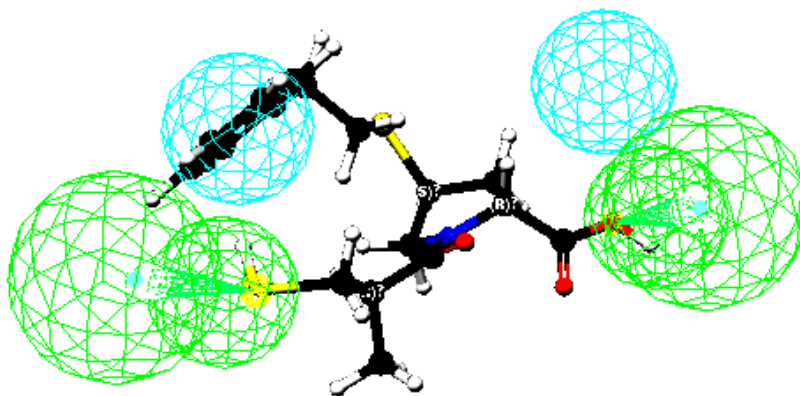
**Fig 1**-Chemical structures of LTA4H inhibitors in the training set together with their biological activity data (IC<sub>50</sub> values, nM) for HipHop run



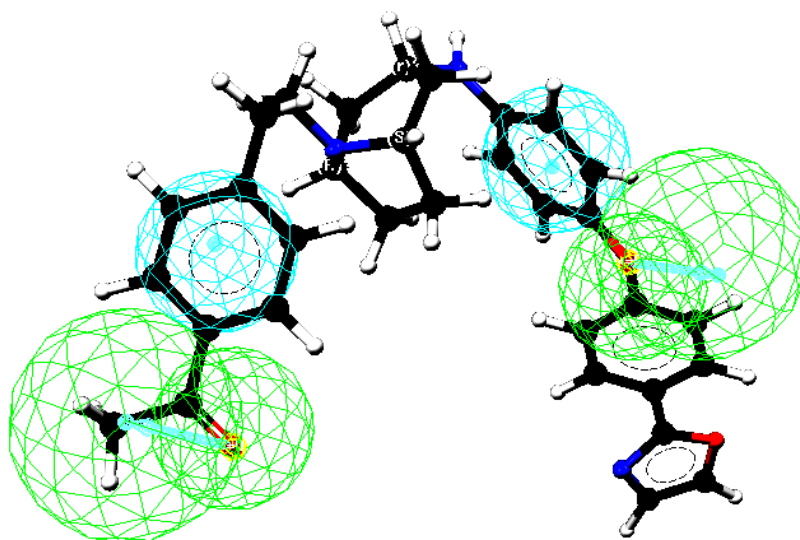
**Fig 2-** The best hypothesis model Hypo 1 produced for the inhibitor molecules of LTA4H protein



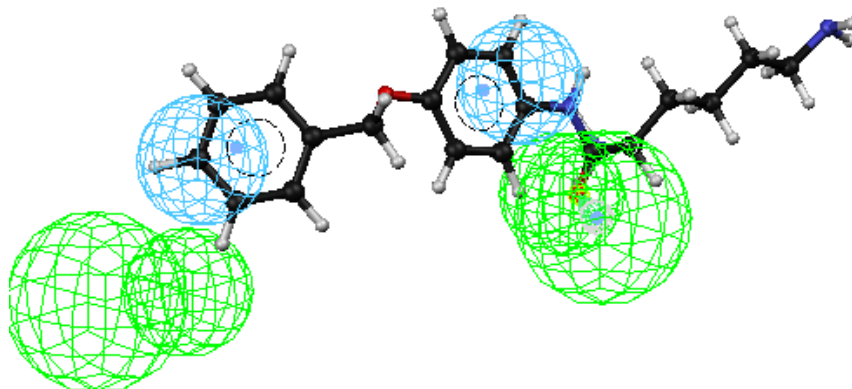
**Fig 3-** Overlapping of highest active inhibitor molecule of training set with the best pharmacophore (Hypo1)



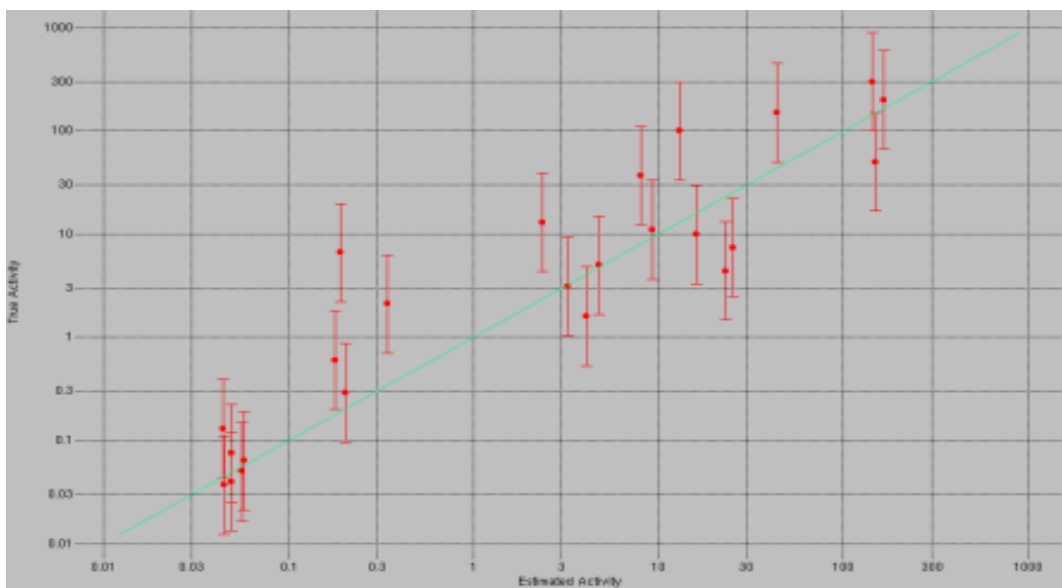
**Fig 4-** Overlapping of lowest active inhibitor molecule of training set with the best pharmacophore (Hypo1).



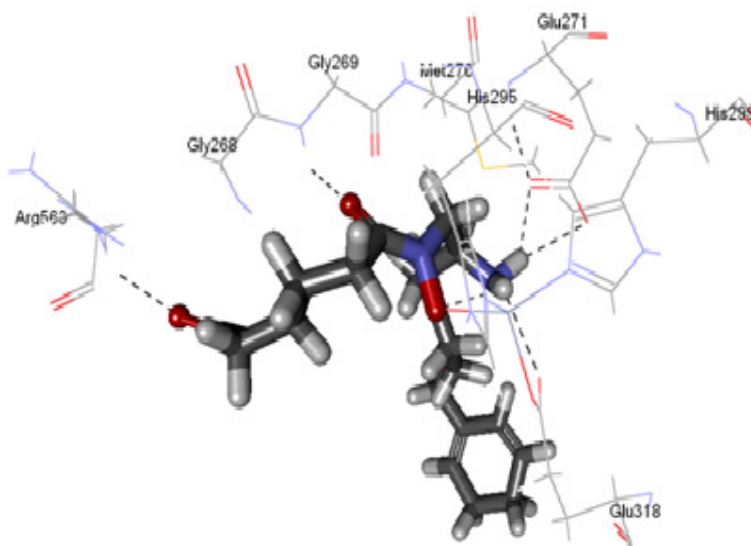
**Fig 5-** Overlapping of highest active inhibitor molecules of test set with the best pharmacophore (Hypo1).



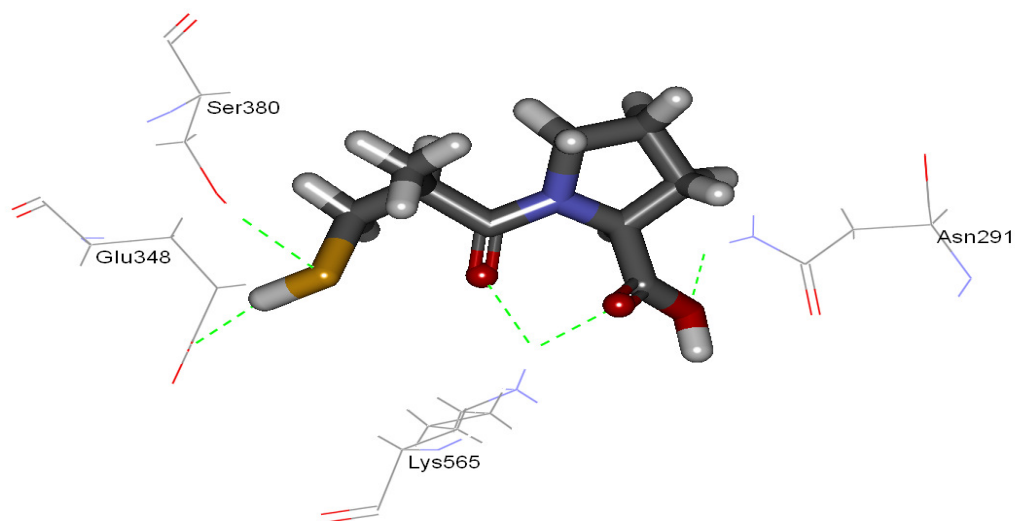
**Fig 6-** Overlapping of lowest active inhibitor molecules of test set with the best pharmacophore (Hypo1).



**Fig 7-** Correlation coefficient of training set molecules is 0.92



**Fig 8-** Highest active molecule (Training set Compound 1) which has been showing its interactions with Gln 136, Gly 268, Gly 269, Glu 271, His 295, Glu 271, Arg563 and His 299 amino acids of protein 2VJ8.



**Fig 9-** Lowest active molecule (Training set Compound 22) which has been showing its interaction with Ser295, Glu348, Asn291 and Lys565 amino acids of the protein 2VJ8.

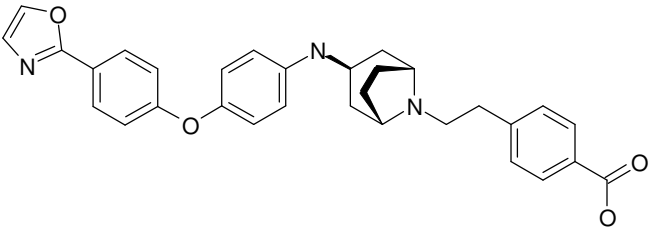
*Table 1-Results of Pharmacophore hypothesis generated using training set against LTA4H inhibitors*



Hypothesis no	Total cost	Null cost-Total cost	RMS deviation	Features	Test set correlation
1	105.148	53.62	1.0867	HA, HA, HPAr	0.920983
2	106.227	52.541	1.14147	HA, HD, HPAr	0.912111
3	108.264	50.504	1.24082	HA, HD, HPAr	0.8946057
4	108.92	49.848	1.26316	HA, HD, HPAr	0.890624
5	110.013	48.755	1.28036	HA, HD, HPAr	0.887981
6	111.13	47.638	1.34754	HA, HD, HPAr	0.87428
7	111.22	47.548	1.34916	HA, HD, HPAr	0.873982
8	111.81	46.958	1.35583	HA, HD, HPAr, HPAl	0.872958
9	113.49	45.278	1.42164	HA, HD, HPAr	0.85897
10	113.528	45.24	1.40374	HA, HD, HPAr	0.863351

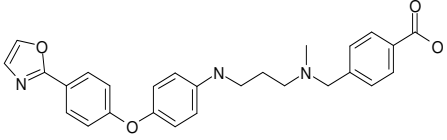
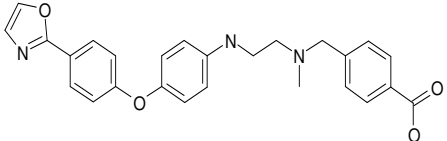
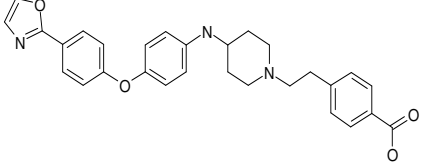
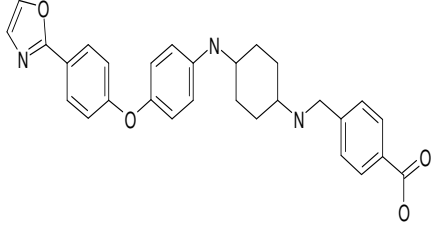
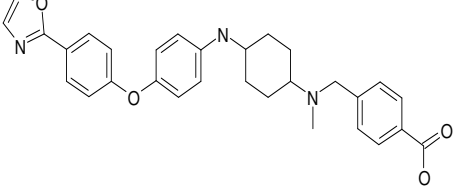
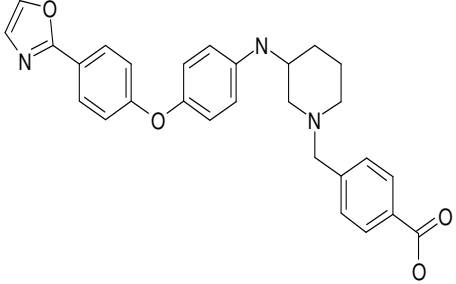
HA- Hydrogen bond acceptor, HD- Hydrogen bond donor, HPAl- Hydrophobic aliphatic, HPAr – Hydrophobic aromatic

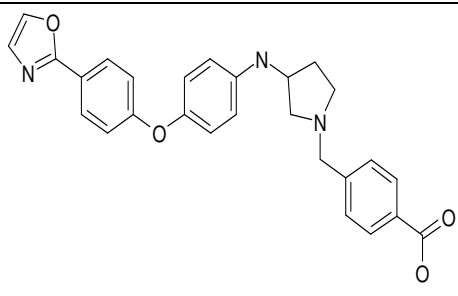
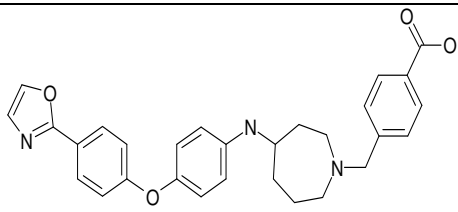
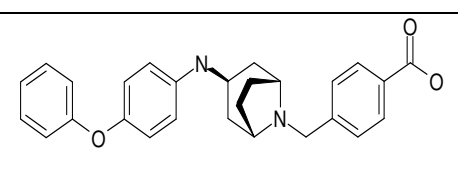
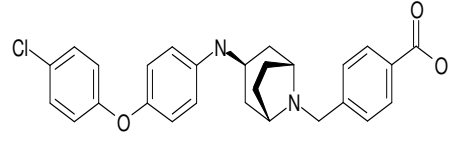
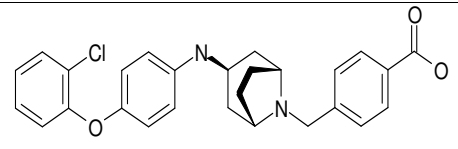
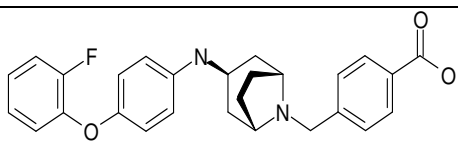
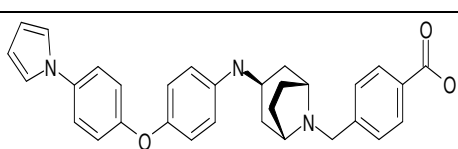
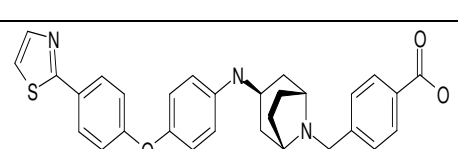
**Table 2-** Docking scores of inhibitors molecules of LTA4H obtained after subjecting to CDOCKER

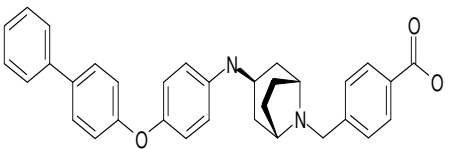
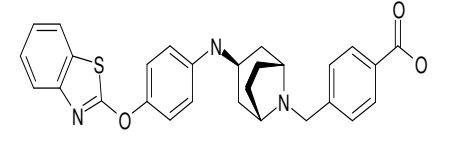
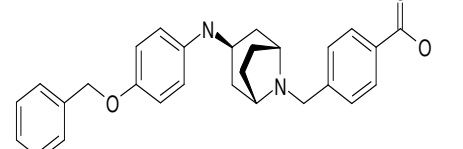
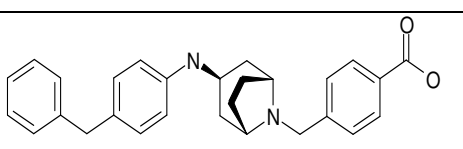
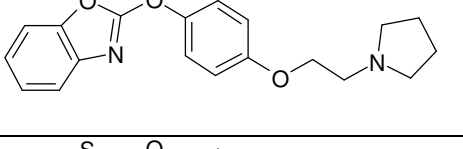
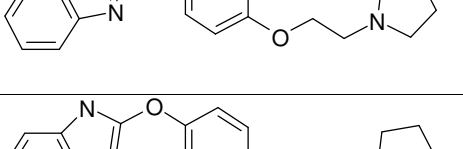
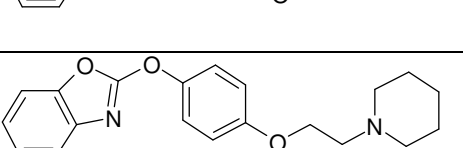
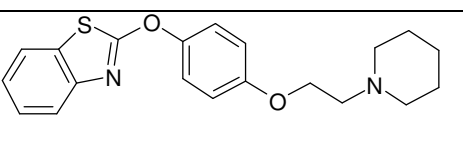
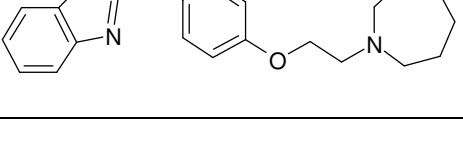

Compound	IC <sub>50</sub> (nM)	Docking score
Highest active		
	1.00	-35.89
Lowest active		

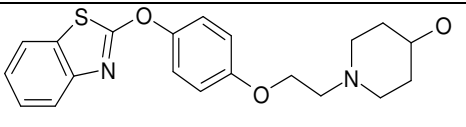
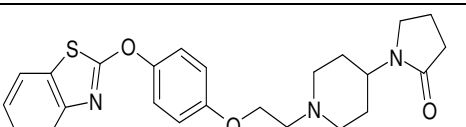
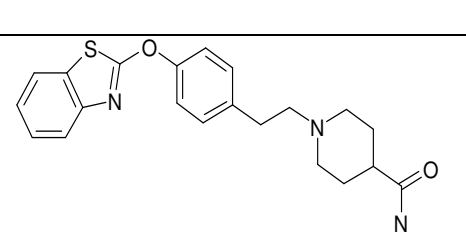
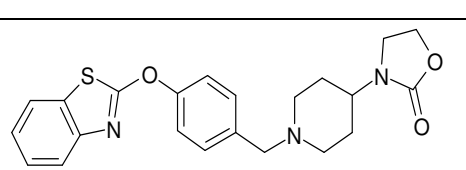
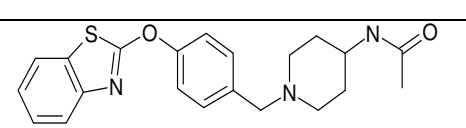
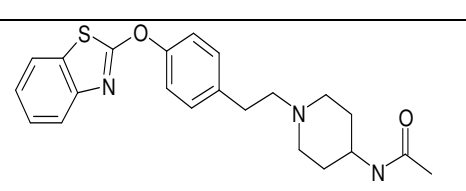
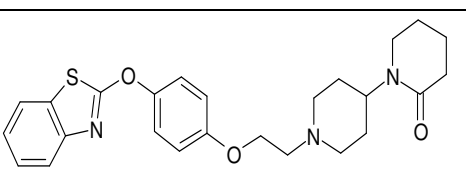
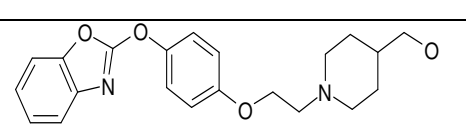
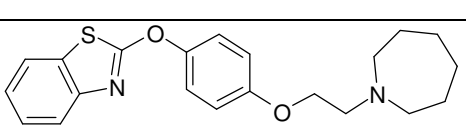
Analog based pharmacophore strategy to identify novel leukotriene a4 hydrolase (LTA4H) inhibitors

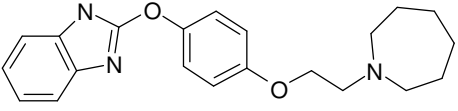
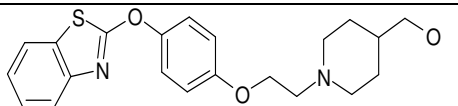
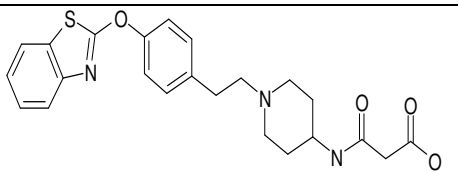
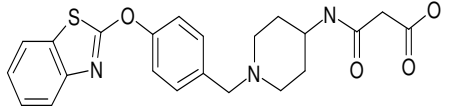
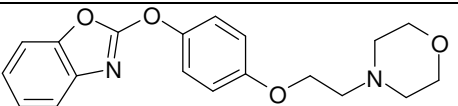
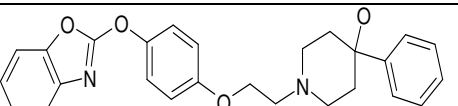
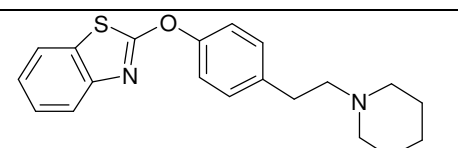
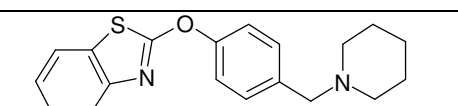
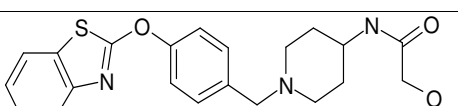
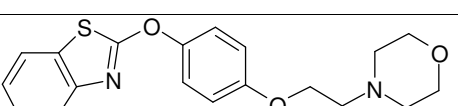
	630000	-13.68
---	--------	--------

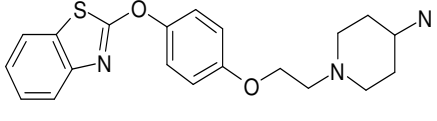
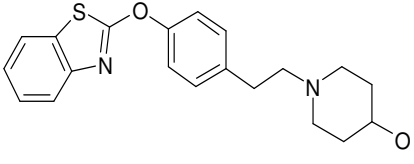
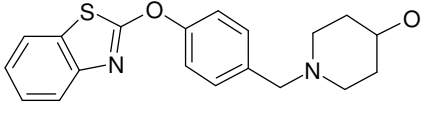
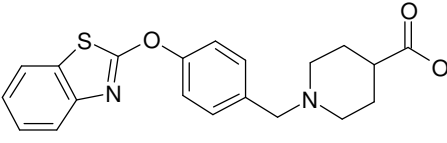
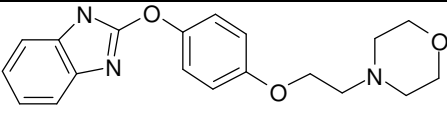
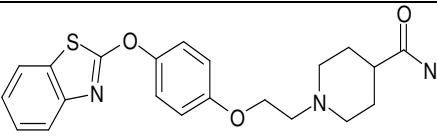
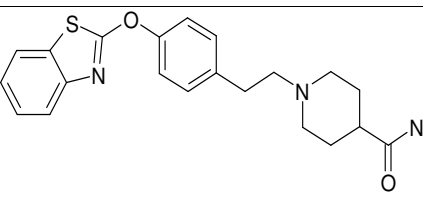
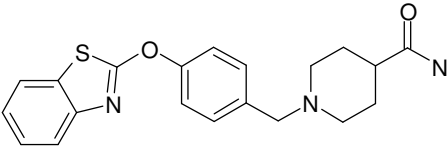
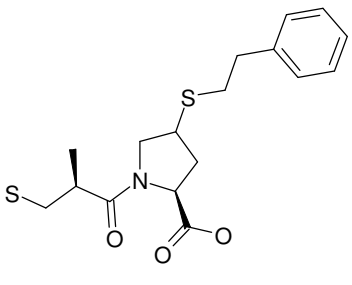
Sr. no	Structure	Experimental $IC_{50}$	Predicted $pIC_{50}$
1		8.522879	7.744727
2		6.886057	8.161151
3		8.522879	8.30103
4		7.958607	8.187087
5		8.045757	8.657577
6		7.221849	8.070581

7		8.154902	7.657577
8		7.823909	8.045757
9		7.853872	6.744727
10		8.221849	7.154902
11		6.49485	7.065502
12		8.221849	7.769551
13		8.39794	8.173925
14		8.09691	7.60206

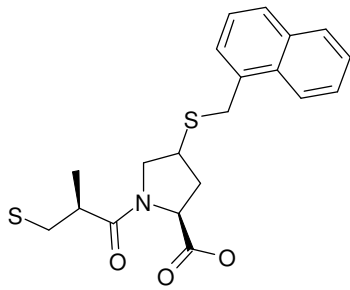
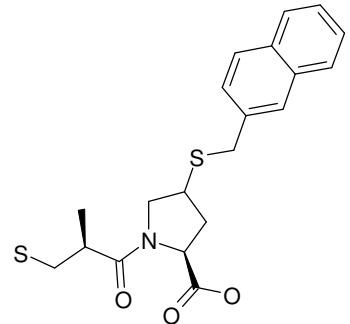
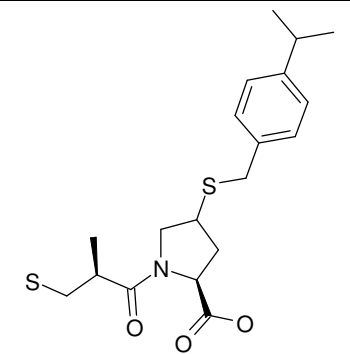
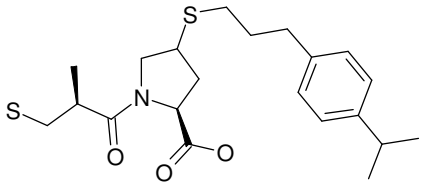
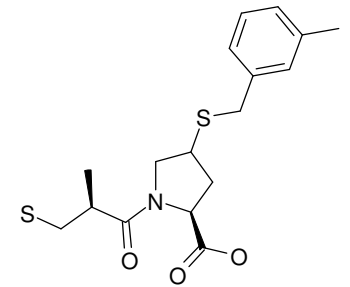
15		8.30103	8.30103
16		8.045757	7.008774
17		7.327902	7.920819
18		8.522879	7.086186
19		8.154902	8.154902
20		7.853872	5.124939
21		7.075721	5.055517
22		7.958607	5.920819
23		7.267606	6.130768
24		8.39794	7.958607

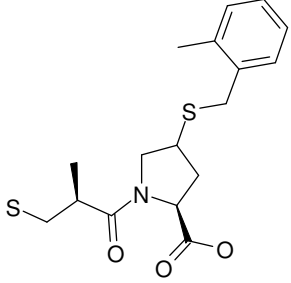
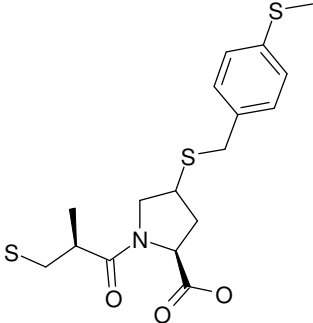
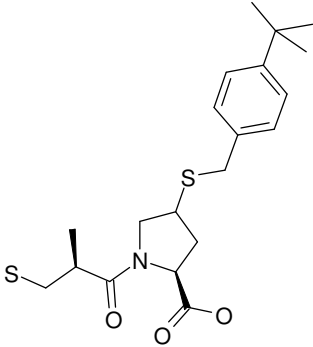
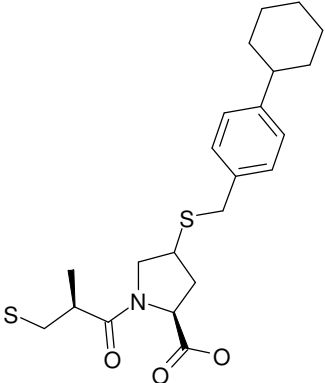
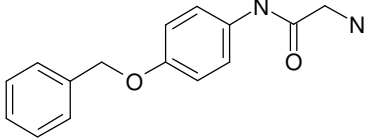
25		7.508638	8.29243
26		7.79588	5.30103
27		7.568636	6.244125
28		8	6.259637
29		7.920819	6.568636
30		7.455932	6.09691
31		7.154902	5.318759
32		7.853872	5.958607
33		7.180456	5.619789

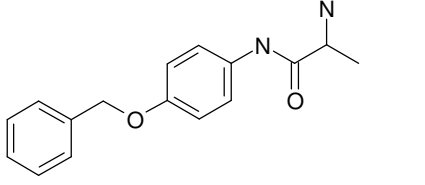
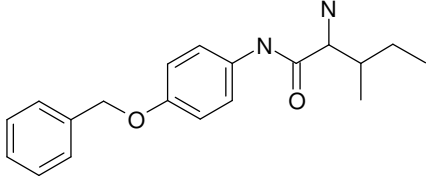
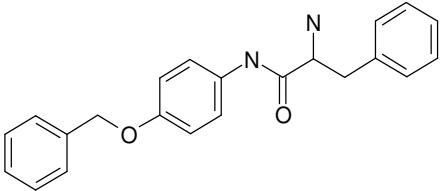
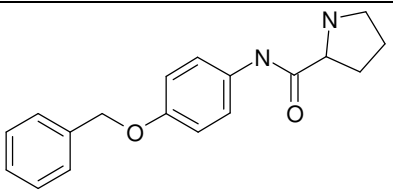
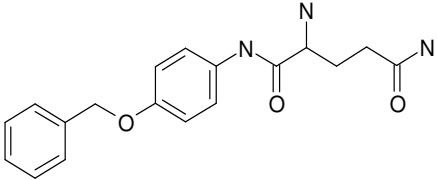
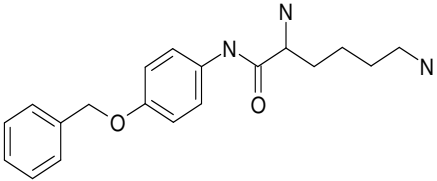
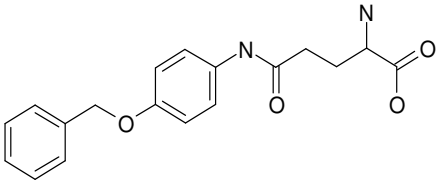
34		6.853872	5.677781
35		7.886057	6.537602
36		7.30103	6.677781
37		7.677781	5.958607
38		7.236572	5.69897
39		8.221849	7
40		7.769551	4.69897
41		7.229148	4.677781
42		8.09691	6.187087
43		6.455932	6.251812

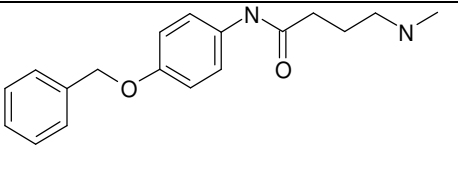
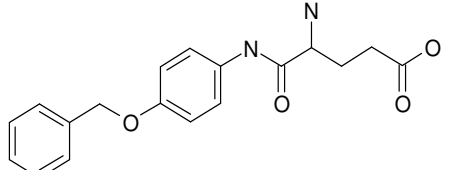
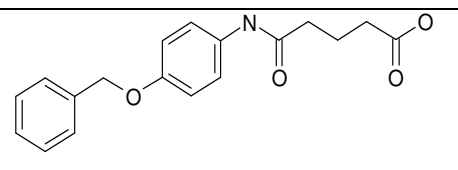
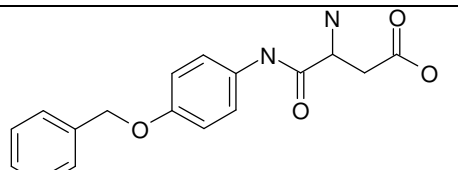
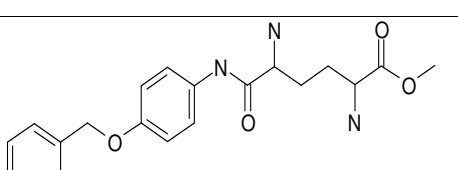
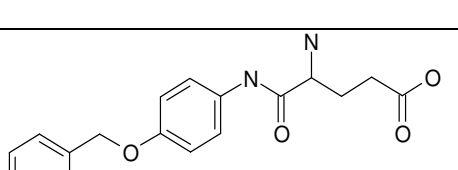
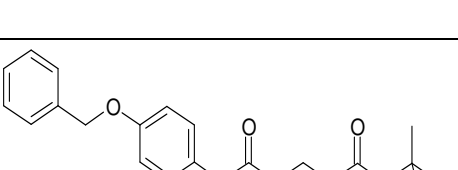
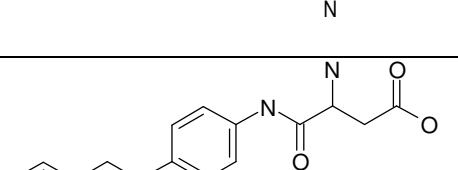
44		7.180456	6.443697
45		8.09691	6.21467
46		7.468521	6.221849
47		7.958607	5.958607
48		5.522879	6.585027
49		7.886057	5.481486
50		7.552842	6.080922
51		7.769551	6.008774
52		5.29243	4.853872

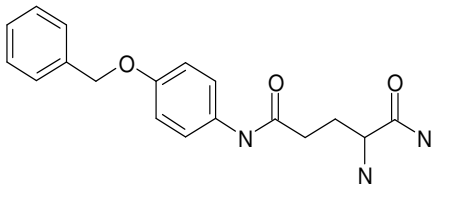
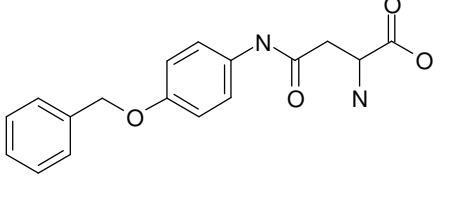
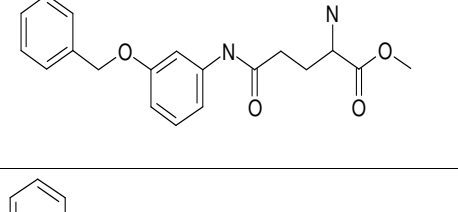
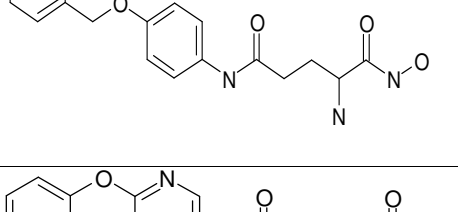
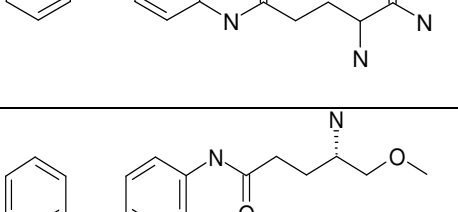
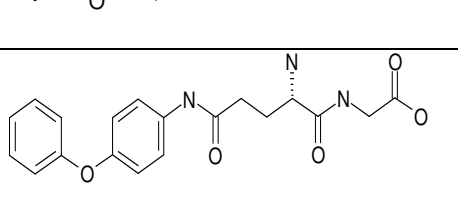
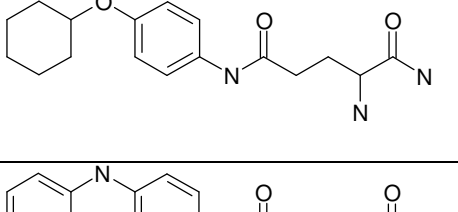
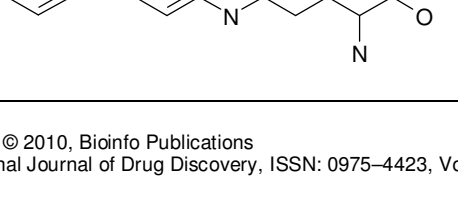



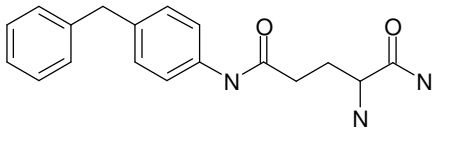
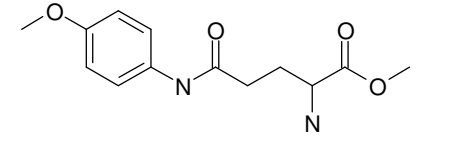
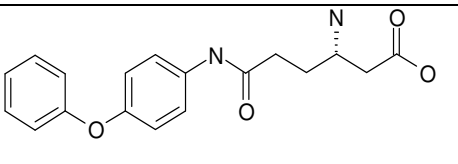
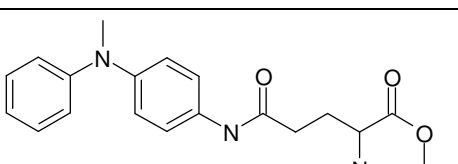
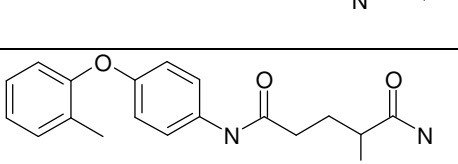
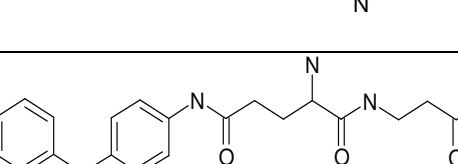
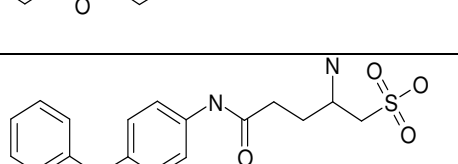
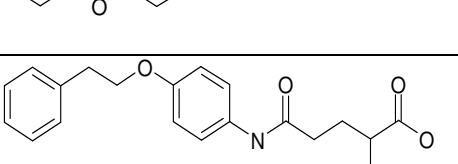
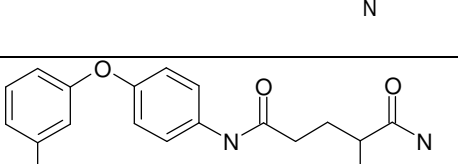
53		5.036212	4.79588
54		5.958607	6.045757
55		7.283997	6.455932
56		5.568636	5.920819
57		5	5.744727

58		6.075721	6.356547
59		6.920819	6.207608
60		7.508638	6.309804
61		7.468521	6.045757
62		6.552842	6.107905

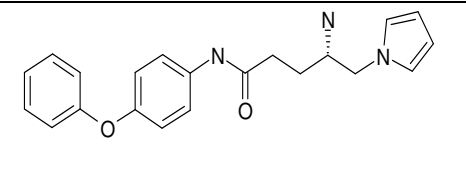
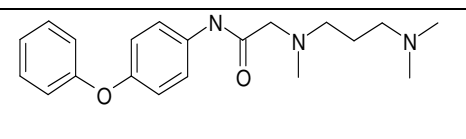
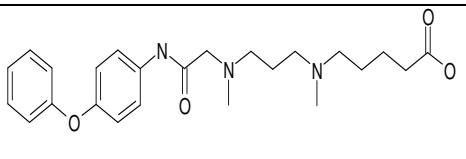
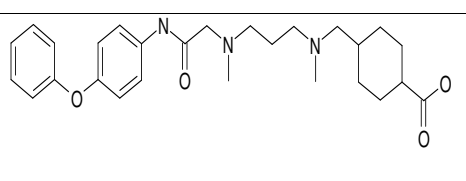
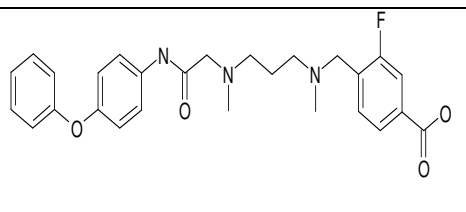
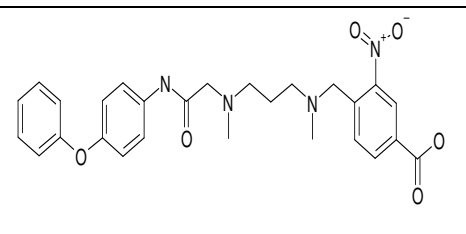
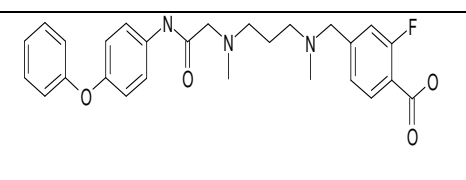
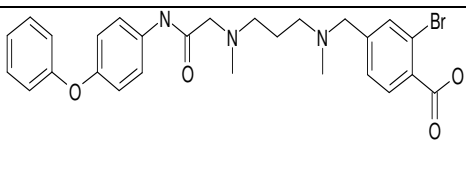
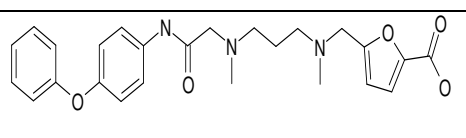
63		6.823909	6.29243
64		5.69897	6.420216
65		5.69897	6.769551
66		5.69897	6.69897
67		5.69897	6.080922
68		5.236572	4.657577
69		5.79588	4.744727

70		4.958607	4.744727
71		6.167491	6.657577
72		4.744727	4.744727
73		5.267606	6.420216
74		7.408935	5.055517
75		5.142668	5.638272
76		7.221849	6.036212
77		5.031517	6.080922

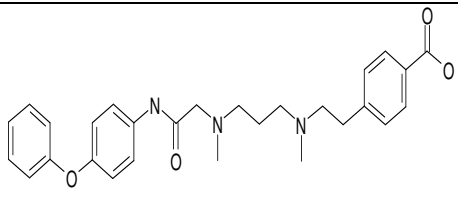
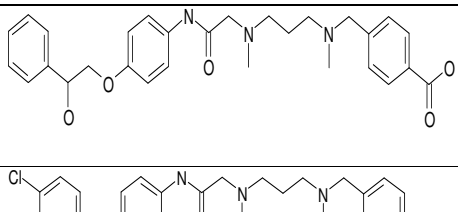
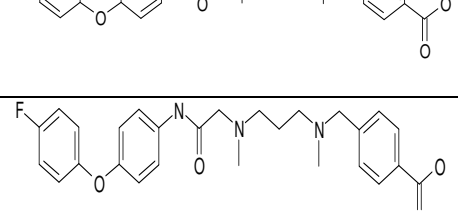
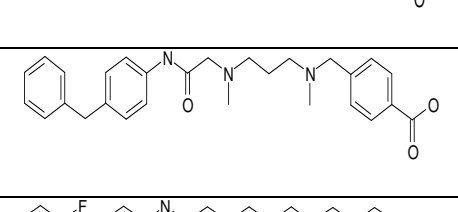
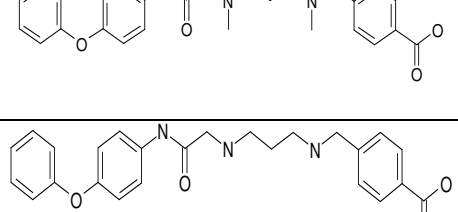
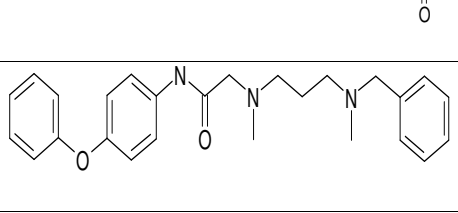
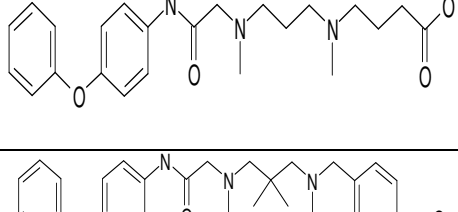

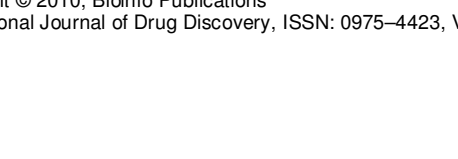
78		7.638272	5.075721
79		5.958607	6.744727
80		6.136677	5.49485
81		7.60206	5.657577
82		5.585027	5.481486
83		5.251812	4.744727
84		7.657577	4.744727
85		4.744727	4.69897
86		6.677781	6.130768

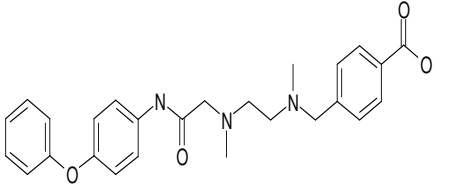
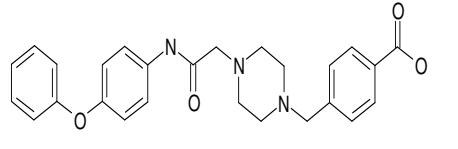
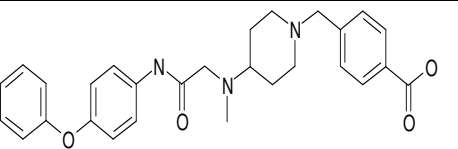
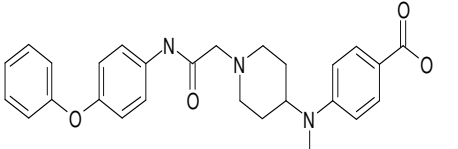
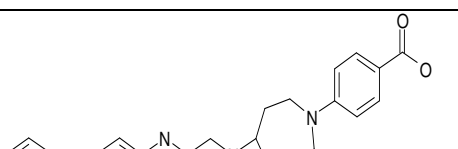
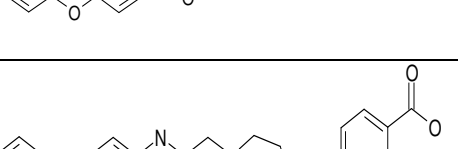
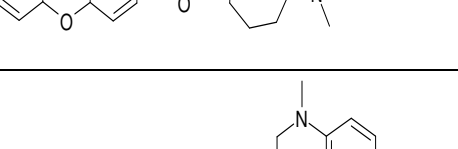
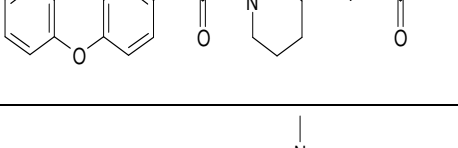
87		7.677781	5.886057
88		4.744727	5.275724
89		8.221849	4.744727
90		5.09691	6.677781
91		5.552842	4.744727
92		7.769551	4.744727
93		6.886057	6.200659
94		7.337242	6.080922
95		6.823909	4.744727

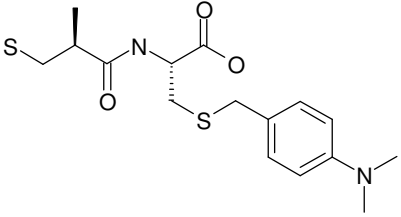
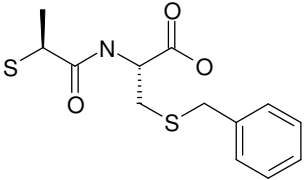
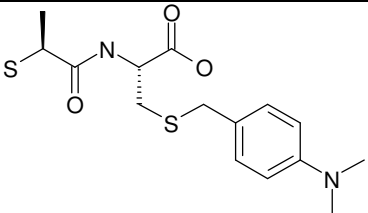
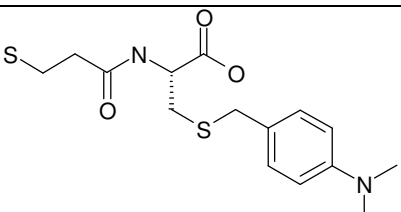
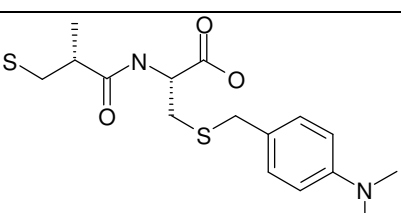
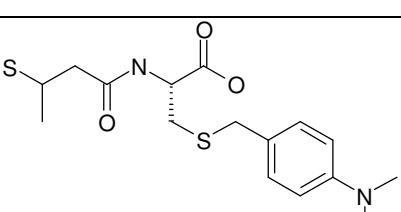
96		7.721246	6.207608
97		6.130768	5.958607
98		6.455932	6.19382
99		7.69897	7.055517
100		7.886057	6.69897
101		7.508638	6.522879
102		7.744727	6.721246
103		7.657577	6.267606
104		7.657577	6.431798

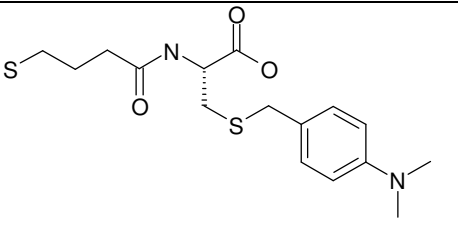
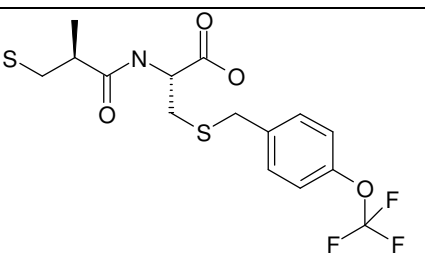
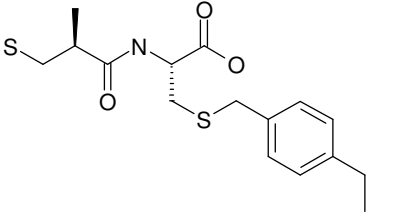
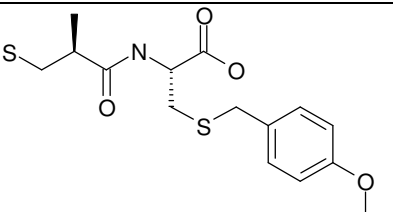
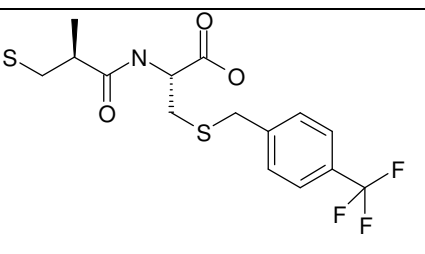
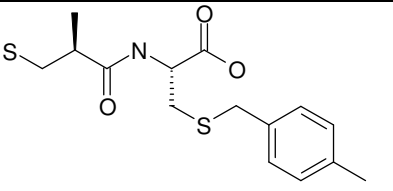
105		6.408935	6.79588
106		6.79588	4.744727
107		7.744727	6.387216
108		7.60206	6.346787
109		8.154902	7.537602
110		7.823909	7.481486
111		8.221849	7.619789
112		8	6.958607
113		7.552842	8.356547

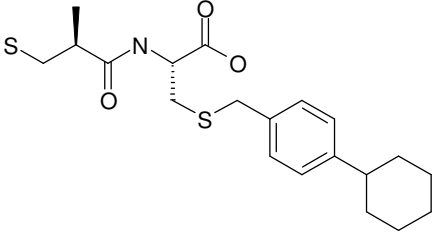
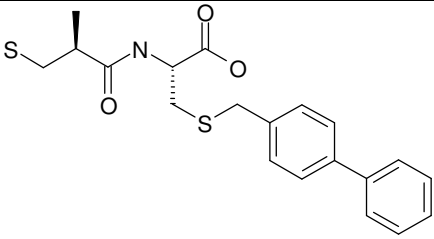
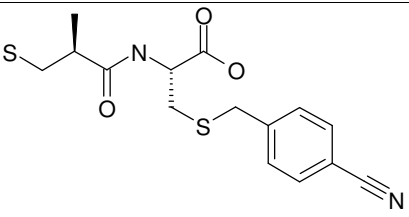
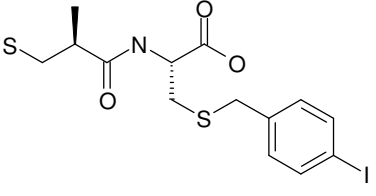
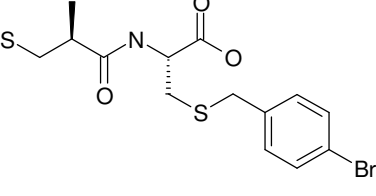
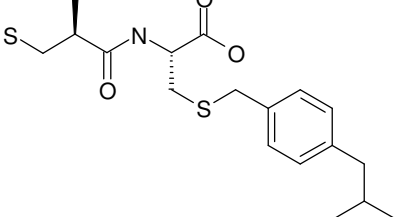


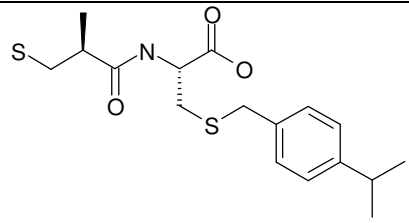
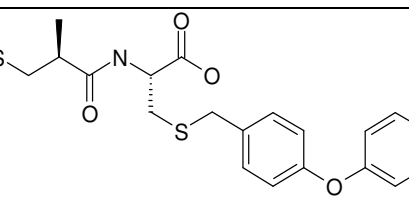
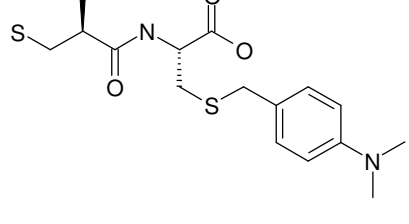
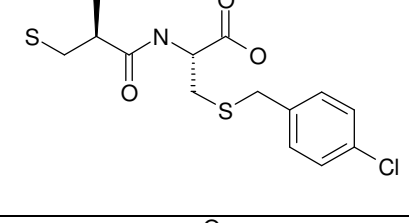
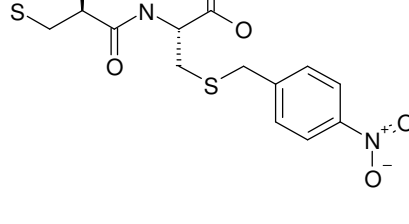
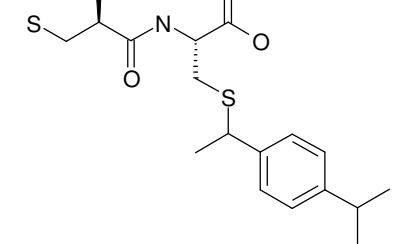
114		8.522879	6.920819
115		7.721246	7.036212
116		7.769551	8.251812
117		8.221849	7.408935
118		8.522879	7.05061
119		7.79588	7.744727
120		6.431798	8.30103
121		7.045757	6.823909
122		5.954677	6.508638
123		8.154902	7.136677

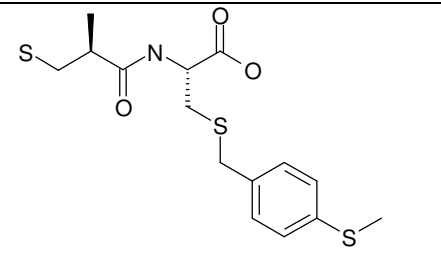
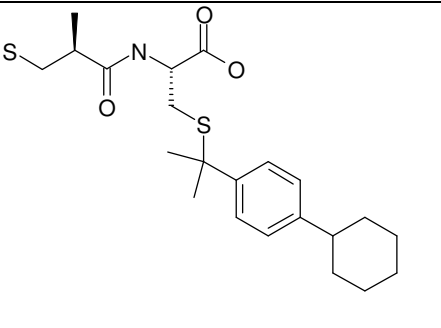
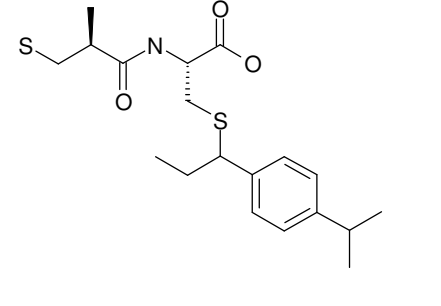
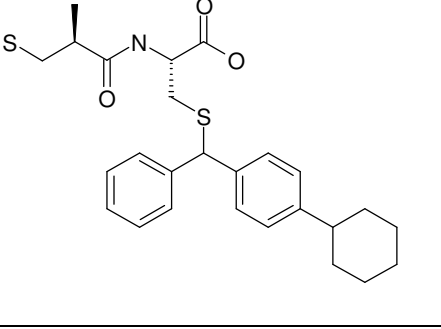
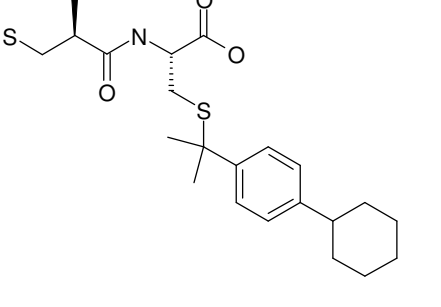
124		7.823909	8.21467
125		6	7.69897
126		7.221849	8.259637
127		6.309804	8.200659
128		6.79588	7.091515
129		6.853872	8.769551
130		7.769551	7.119186
131		7.585027	6.920819

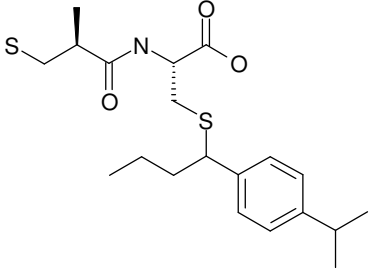
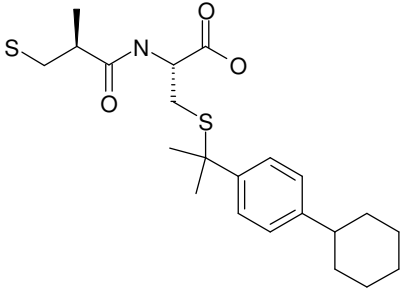
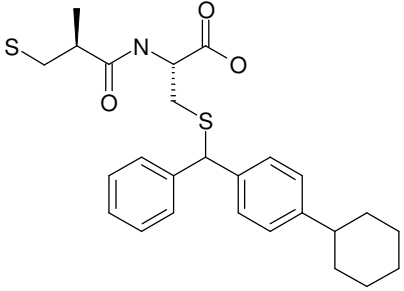
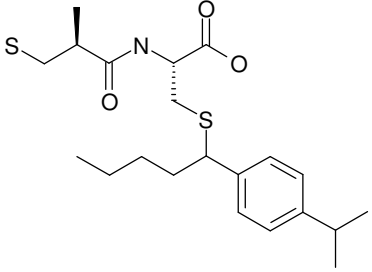
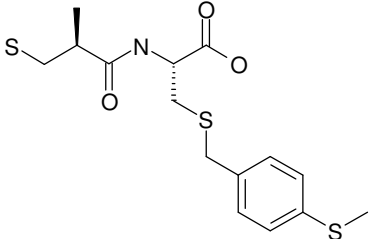
132		6.568636	5.79588
133		5	6
134		5	5.958607
135		5	6.113509
136		5.823909	6.040959
137		5.130768	6.167491

138		5	6
139		6.39794	6.481486
140		6.552842	6.387216
141		5.619789	6.29243
142		6.853872	5.958607
143		5.142668	6.657577

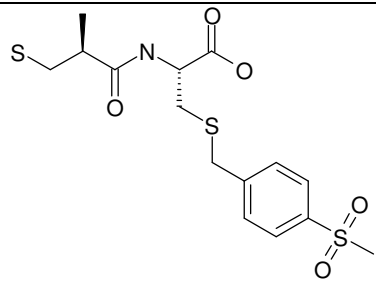
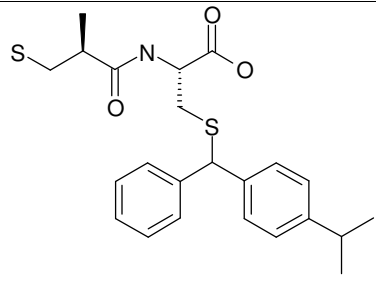
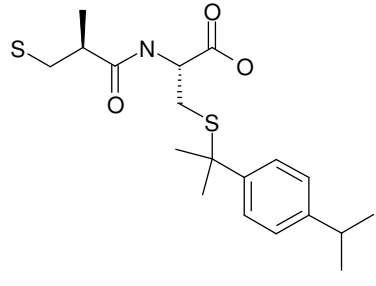
144		7.102373	5.853872
145		6.221849	4.744727
146		6.275724	6.148742
147		7.823909	6.387216
148		6.21467	6.619789
149		7.619789	6.167491

150		5.69897	4.721246
151		5.769551	6.552842
152		5	5.886057
153		5.769551	6.080922
154		5.309804	5.769551
155		7.259637	4.886057

156		7.337242	5.744727
157		7.259637	6.318759
158		7.173925	6.229148
159		6.677781	6.075721
160		7.259637	4.638272

161		6.744727	4.886057
162		7.259637	6.318759
163		6.677781	6.086186
164		6.29243	4.619789
165		7.337242	5.920819



166		6.79588	4.69897
167		7.040959	5.221849
168		7.102373	4.886057